ELSEVIER

Biophysical Chemistry 133 (2008) 1 – 10

Biophysical Chemistry

http://www.elsevier.com/locate/biophyschem

Self-aggregation of free base porphyrins in aqueous solution and in DMPC vesicles

Suzana M. Andrade [a,*], Raquel Teixeira [a], Sílvia M.B. Costa [a], Abílio J.F.N. Sobral [b]

[a] *Centro de Química Estrutural, Complexo 1, Instituto Superior Técnico, Technical University of Lisboa, 1049-001 Lisboa, Portugal*
[b] *The Chemistry Department, University of Coimbra, Rua Larga, 3004-535 Coimbra, Portugal*

Received 19 July 2007; received in revised form 9 November 2007; accepted 10 November 2007
Available online 22 November 2007

Abstract

Free base porphyrin (PPhe), derivatized with aminosulfonyl groups linked to the aromatic amino acid phenylalanine at the *meso*-positions, was mixed with DMPC vesicles. The resulting interaction was studied by absorption, steady-state and transient state fluorescence, at different pHs.

At pH=2 to pH=9, the aforementioned porphyrin predominates as an aggregated species, with a co-facial arrangement of the molecules taking into account the blue shift of the Soret band (414 nm for the monomer and 401 nm for the aggregate). Upon interaction with DMPC vesicles, the competing hydrophobic interactions with the bilayer destabilize the aggregated species in favor of monomer incorporation. Fluorescence lifetimes also show that the long component assigned to the monomer contributes only 30% to the overall decay in solution (e.g. pH=7.0) whereas in DMPC vesicles this contribution increases up to 85% independent of the solution pH, which confirms a location of the probe in an environment "protected" from free water.

The picture changes completely in the case of TSPP, an anionic porphyrin which does not incorporate in DMPC vesicles. Remarkably, at pH=2.5 all the experimental findings point to the self-assembling of the porphyrin units in J-aggregates induced at the surface of the DMPC vesicle. In fact, upon removal of the aqueous solvent, we could define by fluorescence lifetime imaging microscopy (FLIM) regions where the fluorescence lifetime is that characteristic of the J-aggregate ($<\tau_F>$ 0.11 ns).
© 2007 Elsevier B.V. All rights reserved.

Keywords: Porphyrins; DMPC vesicles; J-aggregates; Fluorescence; FLIM

1. Introduction

Porphyrins, as prosthetic groups of enzymes and carrier proteins are important to perform several functions. For example, porphyrins participate as electron transporters in oxidation–reduction processes of cells, in oxygen transport and storage.

Porphyrins and their analogues are known to self-aggregate which is facilitated by a flat, wide, and electron-rich surface, creating van der Waals, π–π stacking, charge-transfer interactions. Porphyrin aggregates also play specific roles in nature namely in photosynthetic plants and in organisms and have potential uses as nonlinear optical materials. In fact, much of the development in molecular electronics has been derived from attempts to mimic the highly efficient electron and energy transfer processes which take place in the light-harvesting complexes and reaction centers of photosynthetic organisms [1,2].

A variety of factors can influence the extent of self-association including the nature of the porphyrin itself (metal ion, number and nature of peripheral groups) as well as external changes as ionic strength, pH, solvent nature, temperature, among others.

A special interest has lied upon strongly coupled aggregates with delocalized excitonic states due to their potential applications as nonlinear optical materials [3,4]. According to Kasha's exciton theory, J-aggregates are formed when the transition dipole moments of the monomer molecules are aligned parallel to the line that joins the molecular centers in the aggregate ("head-to-tail"). By contrast, in the case of H-aggregates, the transition dipole moments of the monomer molecules are perpendicular to the line of centers ("face-to-

* Corresponding author. Tel.: +351 21 8419389; fax: +351 21 8464455.
E-mail address: suzana.andrade@ist.utl.pt (S.M. Andrade).

0301-4622/$ - see front matter © 2007 Elsevier B.V. All rights reserved.
doi:10.1016/j.bpc.2007.11.007

face") [5]. It is generally accepted that a red shift in the electronic absorption spectra relatively to that of the monomer is proof of J-aggregate whereas a blue shift is proof of H-aggregates. Nevertheless, these two types are ideal cases which provide indications regarding the monomers' self-assembling in the aggregate.

Although in literature J-aggregates are especially reported relatively to molecules belonging to the carbocyanine family [6–8], a significant body of investigation in this matter has been devoted to the water-soluble ionic *meso*-tetra(*p*-sulfonatophenyl) porphyrin, TSPP [9–11]. The latter was reported to form, under suitable conditions of pH (below 1) and ionic strength, homo-associated arrays stabilized through a hydrogen bond network acting between the anionic sulfonate groups and the charged protonated nitrogen atoms [12,13]. The coherence length, *i.e.* the number of molecules collectively excited, has been reported to be 5–7, although evidence for a much larger physical size has been given from light scattering techniques [14–16].

This process of aggregation has been reported to be more efficient when the porphyrin interacted with templates such as: proteins [17–19], surfactants [20], microemulsions [21,22], and dendrimers [23] among others. Moreover, in some of these systems both the size and the type of aggregates could be tuned and in fact, H-aggregates were also detected.

Only more recently, the evidence of J-aggregation was reported for another water-soluble porphyrin *meso*-tetra(*p*-carboxyphenyl) porphyrin, TCPP, in very acidic conditions which was counterion dependent [24].

The present work encompasses a new class of sulfonamide *meso*-tetraphenylporphyrin derivatives linked to amino acid phenylalanine groups — *PPhe*, Scheme 1. Besides the terminal carboxylic groups similar to TCPP, Phe contributes to increase the dye hydrophobicity which were shown determinant for incorporation in liposomes. The sulfonamide group, known to be present in many drugs with bactericide and chemotherapeutic applications [25], may contribute to molecular association/dissociation through intra-/intermolecular hydrogen bonding. In fact, the existence of small aggregates was reported for PPhe in AOT RM, dependent on the amount of water present in the system [26].

We have investigated and report herein, the influence of the microenvironment provided by DMPC bilayer vesicles in the self-aggregation pattern of the aforementioned porphyrins, TSPP and PPhe. These vesicles can be considered as a close model of biological membranes which offer the advantage of being thermodynamically stable and easily reproducible. The importance of understanding the interactions of these self-organized nanoscale molecular assemblies with porphyrins are stressed by their potential application in molecular photonics and artificial photosynthesis.

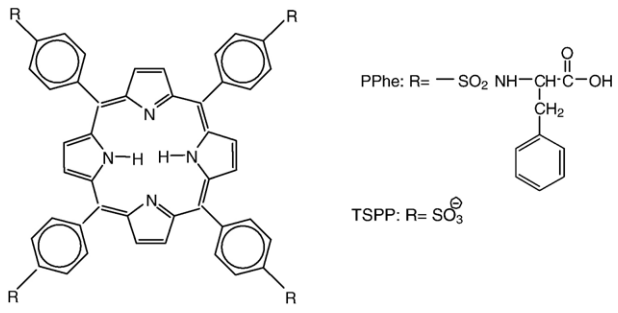

Scheme 1.

We will report spectroscopic evidence for a complex pattern of PPhe aggregation in water at different pHs that simplifies in the presence of DMPC vesicles where essentially monomers are incorporated. By contrast, TSPP exists as a monomer in water which does not incorporate in DMPC bilayers. In the zwitterionic form, TSPP aggregates at the vesicle surface which is well supported by fluorescence lifetime imaging.

2. Experimental

2.1. Materials

The porphyrin *meso*-tetra (phenylalanine-4-amino sulfonylphenyl) porphyrin (PPhe) was synthesized and purified as described elsewhere [27]. TSPP was obtained from Fluka ≥98% purity (catalogue no. 88074). 1,2-Dimirystoyl-*sn*-glycero-3-phosphocholine (DMPC) >99% purity was obtained from Avanti Polar Lipids (Alabaster, AL, USA). Buffer solutions were made up with bidistilled water, following the recommended procedures. The buffer citrate–(sodium)phosphate was employed for pH=2.5 to 7.0, and the more acidic pH or more alkaline pH were obtained by adding a few drops of highly concentrated solutions of HCl and NaOH, respectively. The buffer concentration was 25 mM. All solvents were spectroscopic grade.

2.2. Vesicle preparation

Phospholipid vesicles were prepared at concentrations between 0.01 and 0.8 mM. The appropriate amount of phospholipid was dissolved in a chloroform/methanol 2:1 v/v mixture (~100 μL). The solvent was evaporated under a nitrogen stream to obtain a thin lipid film. Residual solvent was removed under vacuum overnight. The flask containing the lipid film was placed in a warm water bath (with the temperature above the phospholipids main phase transition, T_m=24 °C at pH≥6 and T_m=27.5 °C at pH=2.5) and the film was hydrated with the citrate–phosphate buffer of desired pH under mild agitation. To obtain the vesicles the hydrated phospholipid dispersions were extruded using a LiposoFast Basic mini-extruder (Avestin, Ottawa, Canada) by means of 15× through 0.4 μm pore diameter polycarbonate filters (Whatman, Clifton, NJ, USA) while maintaining the temperature above the main phospholipid phase transition. The liposomes were then stored at 4 °C and incubated at working temperature for at least 1 h before usage. Stock PPhe solutions were prepared in acetone, the desired volume of this solution was evaporated and mixed with 5 mL of buffer solutions. The final porphyrin concentrations used in this work were in the range $0.1–1.10^{-6}$ M. The size distribution of the vesicles was obtained using a multi-angle Brookhaven Instruments (BI-200SM goniometer and a BI-2030AT autocorrelator) with a He–Ne laser (632.8 nm,

35 mW) from Spectra Physics (model 127) under controlled temperature, $T=32\pm1$ °C. A relatively monodisperse population (polydispersity ≤ 0.17) was obtained at both pH=2.5 and pH=7, with an average hydrodynamic diameter, $D_H=340\pm8$ nm at pH=7 (similar to that in water) and $D_H=145\pm2$ nm at pH=2.5 with an observation angle of 90°. The value obtained at pH=2.5 may not be associated to smaller vesicles but rather to changes in shape since a dependence on the observation angle was detected [28].

2.3. Photophysical studies

UV–Vis absorption spectra of the samples were measured using a Jasco V-560 spectrophotometer (Easton, MD, USA) and, when necessary, corrections for turbidity were carried out. [29] CD spectra were obtained with a Jasco spectropolarimeter J-720 with spectral averaging and baseline correction. The studies have been performed at a constant TSPP concentration of 2 μM in the visible range and varied DMPC concentration All cells used were quartz with 1 cm pathlengths and temperature was maintained at 32.0±0.2 °C in a thermostated chamber by using a circulating water bath.

Steady-state fluorescence measurements were performed with a SPEX® Fluorolog spectrofluorimeter with a FL3-11 configuration (HORIBA Jobin Yvon). The instrumental response at each wavelength was corrected by means of a correction function provided by the manufacturer.

Fluorescence decays were obtained with a time-correlated single-photon counting (TC-SPC) technique using commercial equipment Microtime 200 from Picoquant GmbH described elsewhere [30]. Briefly, the measurements are performed in front-face geometry and the backscattered light is attenuated through the use of appropriate filters. Excitation was achieved using a pulsed laser diode head at 405 nm or 638 nm, with varied repetition rate (10, 20 or 40 MHz). The maximum output power is 0.4 mW and a minimum pulse width of 54 ps is obtained. A band-pass filter with a transmission in the range 600–800 nm (for 405 nm excitation) or a 695/55 (for 638 nm excitation) was used to eliminate backscattered light in the photomultiplier tube from Picoquant (model PMA-182). Data acquisition can be recorded with 4096 channels per range with a time increment smaller than 40 ps. Data analysis was performed by a deconvolution method using a nonlinear least-squares fitting program, based on the Marquardt algorithm. The goodness of the fit was evaluated by the usual statistical criteria and by visual inspection of the distribution of weighted residuals and the autocorrelation function. Fluorescence Lifetime Imaging was performed in the same setup and a more detailed description may be found elsewhere [31].

3. Results

3.1. Self-aggregation properties of PPhe induced by pH changes

PPhe solubility in aqueous solutions is highly dependent on the solution pH which is related to changes in the porphyrin ionization state and the porphyrin tendency to self-aggregate. At pH=0.8, the absorption spectra show only two Q-bands (Table 1) characteristic of the porphyrin with their pyrrole nitrogens protonated, which is also reflected in a single fluorescence band centered at ~674 nm. However, the absorption Soret band is quite broad ($\lambda_{max}\sim442$ nm) and different from the excitation spectra obtained by collecting emission at 670 nm (or at 640 nm). The latter show a narrow (fwhm ~950 cm^{-1}) Soret band centered at 435 nm, common to the protonated free base porphyrins. This puts into evidence the existence of nonfluorescent aggregates which absorb essentially in the red portion of Soret band. The contribution of such aggregates decreases as the solution pH is raised until no contribution from the diprotonated porphyrin is detected (*i.e.* until pH=5). The emission decays (Table 2) show a bi-exponential behavior with a long lifetime $\tau_F\sim3.3$ ns as the major contribution similar to that obtained for the diprotonated form of TSPP and a shorter one ($\tau_F\sim0.6$ ns) with increasing contribution upon pH raise in the range 0.8–4, as we will discuss below.

At pH=2–4 there are some solubility difficulties which are reflected in a drastic decrease in the absorbance and fluorescence intensity. The splitting of the Q-band absorption and emission also observed hints for the presence of a neutral form. Moreover, excitation spectra obtained at 640 nm or 670 nm no longer coincide and are much broader (fwhm ~2500 cm^{-1}). The former shows more of species absorbing with maximum around 420 nm which indicates that neutral forms are already present contributing to solubility decrease. A blue-shifted absorption is also denoted around 405 nm which is associated to red-emission (~670 nm). The formation of aggregates and the consequent light scattering from the solutions on increasing pH in this range prevent a quantitative analysis of titration curves and thus the estimation of the pK_a for the protonation of the nitrogen atoms.

By raising the temperature, at pH=3, Fig. 1A, the aggregation is disfavored, and indeed, the species absorbing more to the blue is destabilized and fluorescence emission is enhanced.

Table 1
Absorption peaks, Soret bandwidth and fluorescence emission maxima of PPhe in different media, ([DMPC]=0.25 mM; [HSA]=25 μM; λ_{exc}=415 nm; T=32.0 °C)

pH	Absorption maxima/nm					fwhm[a]/ cm^{-1}	Emission max./nm	
	Soret		Q-bands					
0.8	442	–	–	598	648.5	2860	675	–
2.0–4.0	419.5 (405)	516.5	551	n.d.	n.d.	2890	666.5	715
5.0–9.0	401 (415)	517	553	591	644	1880	669 (655)	716
DMPC pH=3.0	418	517	548	587	n.d.	850	649.5	715
DMPC pH=7.0	418.5	516.5	547.5	589	n.d.	904	651	716
HSA pH=3.0	420.5	516.5	544	593.5	n.d.	885	650.5	716.5
HSA pH=6–9	419	516	551	590	n.d.	930	648.5	715
DMSO	419	514	548	588	642	825	650.5	716

Underlined values correspond to the peaks with maximum fluorescence intensity.
[a] Full width at half maximum.

Table 2
Fluorescence lifetimes of PPhe in different media

Medium	A_1 (%)	τ_1/ns	A_2 (%)	τ_2/ns	A_3 (%)	τ_3/ns	χ^2
Buffer pH=1.0 [a]	68	3.53	–	–	32	0.61	1.09
Buffer pH=3.0 [a]	15	4.73	–	–	85	0.61	1.09
Buffer pH=4.0 [a]	5.5	5.42	23	1.00	71	0.55	1.09
Buffer pH=7.0 [a]	30	11.76	12	2.66	41	0.70	1.09
DMPC pH=3.0 [b]	85	11.90	9	4.32	6	0.82	1.07
DMPC pH=7.0 [b]	79	11.86	9	4.40	12	0.81	1.05
DMSO [a]	92	11.09	8	2.85	–	–	1.10
HSA pH=7.0 [b]	99	12.10	1	3.61	–	–	1.10

λ_{exc}=405 nm; T=25 °C.
[a] [PPhe]=1 μM.
[b] [PPhe]=0.1 μM.

The contribution of the short lifetime, $\tau_F \sim 0.6$ ns, is promoted at these pHs together with an increase in the long component lifetime, Table 2. Moreover, in the pH range of 4 to 5, the fluorescence decays would be more accurately described by a distribution model than with the discrete exponential one where both pre-exponential as well as lifetime components are changing.

Upon pH increase from pH=5 up to pH=9, we observe gradual changes which follow a similar pattern. An increase in solubility is detected by absorbance and fluorescence intensity increase more pronounced at pH=5–6 which probably coincides with the changes in peripheral carboxylic groups protonation. As in the case of the diacid species, the determination of the pK_a for this process was prevented by the light scattering of the solutions. For TCPP, a meso-substituted carboxyphenyl porphyrin, these changes occur in the 5–7 pH region (the highest pK_a value reported is at pH=6.6 [32]). Therefore, a tetra-anionic species will tend to be more soluble than a neutral one, the latter prevalent at pH=2–4.

A decomposition of the Soret band by a Gaussian function shows two main contributions: a band centered at 403 nm which prevails in absorption and in excitation (with λ_{em}=670 nm) and another at 415 nm more important in excitation (with λ_{em}= 640 nm). By raising the temperature in this pH region, pH=7 Fig. 1B, we see that the latter is promoted. Moreover, we see an increase in fluorescence intensity and a blue shift (from 667 to 654 nm) and could detect an isoemissive point (not shown). These data clearly suggest a deaggregation process where the aggregated species has a lower fluorescence efficiency than the monomer in which it is converting.

The overall spectroscopic features are consistent with the existence of dimers with an H-type geometry according to excitonic coupling model [5]. As we may see from Table 2, at pH≥6 the lifetimes and the pre-exponentials associated to them do not vary within experimental error: a long component ($\tau_F \sim 11$–12 ns) which can be safely assigned to the monomeric species and an intermediate one ($\tau_F \sim 3$ ns) attributable to a dimeric form, are similar to those obtained in solvents like DMSO; and a short one ($\tau_F \sim 0.7$ ns) which prevails in water where aggregation is more important. Since the close proximity of chromophores in dye aggregates can promote nonradiative decay, thus contributing to fluorescence quenching, the fastest component detected in water may be attributed to PPhe oligomers [33,34]. In the case of bis-glycosamide derivatives of protoporphyrin IX a model was assumed in which a face-to-face dimer of porphyrins (with a lateral offset) is stacked to another one stabilized through a network of hydrogen bonds connecting the lateral glycosamide groups [35]. Another model is proposed for protoporphyrin IX where protonated carboxylic groups are hydrogen bonded to the inner NH [36]. In the case of PPhe we could envisage that possibility for PPhe aggregates at pH below 6. At higher pH, there must be an additional role for the sulfonamide group in minimizing repulsions between the negatively charged groups of neighbor molecules and adding favorable p–p interactions together with possible H-bonding sites.

Pasternack and Collings [37], showed that scattered light could be measured in a conventional spectrofluorimeter and could be related to the extent of electronic coupling between neighbor chromophores in the aggregate and respective size and geometry. The RLS of PPhe resulted in low Rayleigh scattering from the solution and a well due to photon absorption in almost the entire pH region under study (data not shown). Only at pH=0.8–1, a more intense signal to the red of absorption

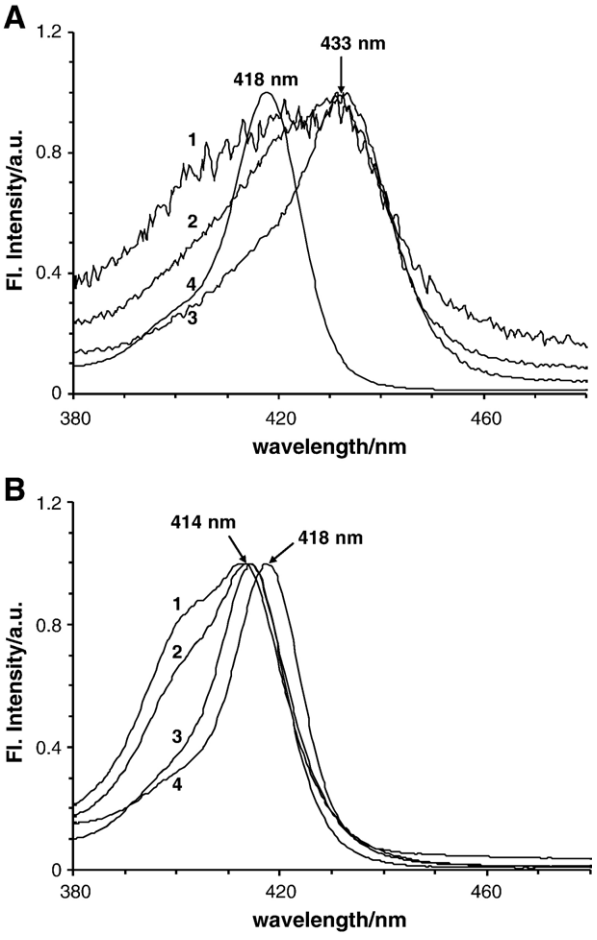

Fig. 1. Normalized fluorescence excitation spectra of PPhe (λ_{em}=640 nm) in aqueous solution and in the presence of DMPC vesicles at (A) pH=3 and at (B) pH=7: 1 — [PPhe]=1 μM and T=32 °C; 2 — [PPhe]=0.1 μM and T=32 °C; 3 — [PPhe]=0.1 μM and T=62 °C; 4 — [PPhe]=0.1 μM, [DMPC]= 0.25 mM and T=32 °C.

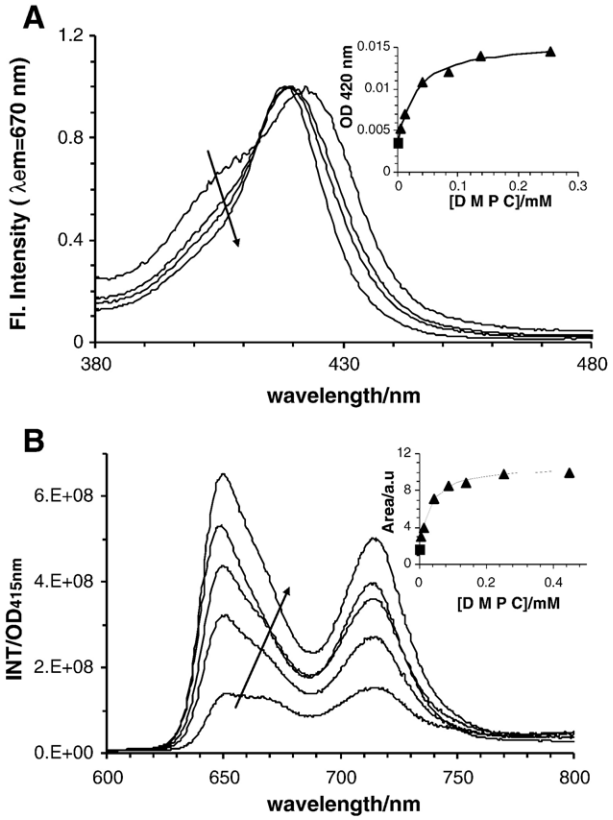

Fig. 2. (A) Normalized fluorescence excitation and (B) emission spectra of PPhe in the presence of increasing [DMPC] shown by the arrows from 0 to 0.45 mM at pH=3.0. Insets: plot of the absorbance at 420 nm and fluorescence integrated spectra of PPhe/DMPC (▲). The full lines represent best fits with Eq. (1).

(~465 nm) was found without any specific resonant peak. According to literature, in the case of TCPP a resonant peak could only be found in aqueous HNO_3 at pH=0.9 [24]; whereas for TSPP J-aggregates, an even sharper and intense resonant peak red-shifted (~499 nm) from that in absorption is observed. According to RLS theory, this means that the structural arrangement of PPhe has a weak electronic coupling, involving only a dimer. For instance, in the case of Protoporphyrin IX no aggregated species could be detected at pH below 1 [36]. The presence of aromatic groups at the *meso*-positions is considered to be necessary for the formation of porphyrin J-aggregates. However, the presence of sulphonamide and phenylalanine groups in PPhe may introduce some steric hindrance and prevent such highly organized molecular arrangement. Furthermore, the zwitterionic nature of TSPP monomers was suggested to contribute with additional Coulombic interactions to stabilize an arrangement with a larger number of interacting chromophores in close association. By opposition, in PPhe the carboxylic groups are uncharged in very acidic conditions, as in the case of TCPP, where a distribution of physical aggregate sizes was reported [24].

3.2. PPhe interaction with DMPC vesicles

The affinity of PPhe towards DMPC vesicles was investigated. For this purpose we followed both the absorption and fluorescence signals of PPhe in the presence of increasing concentrations of DMPC at pH 3, Fig. 2 and pH 7, Fig. 3. The latter was performed at [PPhe]=0.1 μM and 1 μM to evaluate how the presence of aggregates in solution affect the association process.

The results obtained in the presence of DMPC show a similar pattern and at the highest [DMPC] studied the spectra are almost superimposable at both pHs. Likewise, in organic solvents like DMSO or dioxane, an increase in absorbance together with a significant red shift of Soret band maximum is observed. The fluorescence also reflects a similar trend: a slight red shift is detected in the fluorescence maxima. Fluorescence lifetimes obtained for PPhe in the presence of high [DMPC] are also independent of the solution pH.

This suggests that the same PPhe species associates with the lipidic environment of the vesicle which is "protected" from differences in the pH of the aqueous surroundings. At the interface of a phospholipid layer, water is perturbed (the network of H-bonds is modified and thus the properties of interfacial water – density, mobility, lifetime of H-bond – are different from those of free water) by up to 1 nm away from it [38].

At the same [DMPC], the ratio monomer/aggregate is always higher for the lowest [PPhe], pointing for the preferential

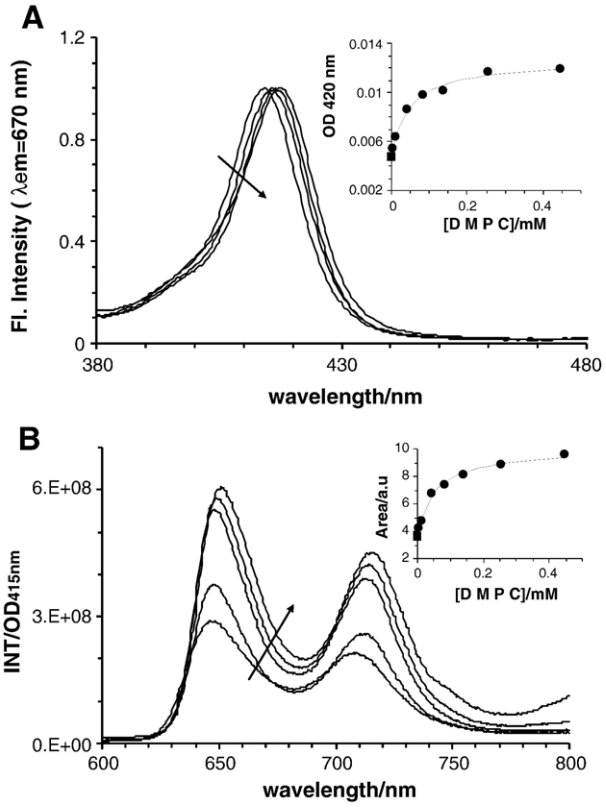

Fig. 3. (A) Normalized fluorescence excitation and (B) emission spectra of PPhe in the presence of increasing [DMPC] shown by the arrows from 0 to 0.45 mM at pH=7.0. Insets: plot of the absorbance at 420 nm and fluorescence integrated spectra (●) of PPhe/DMPC. The full lines represent best fits with Eq. (1).

association of monomeric species with DMPC, which can be rationalized from the following equilibria:

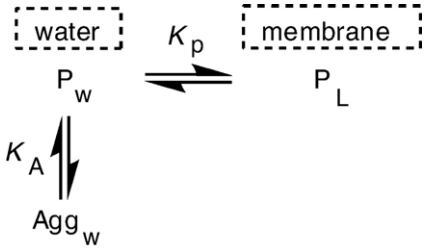

In the presence of DMPC vesicles, the absorbance signal at 422 nm, the emission at 650 nm or fluorescence excitation at 424 nm, increase with increasing DMPC concentrations until reaching a plateau value. This trend can be rationalized by means of the model in which the porphyrin is assumed to distribute between the lipid phase (L) and the aqueous phase (W), with a partition coefficient $K_p=[PPhe]_L/[PPhe]_W$ and an association constant $K_L=K_p/[DMPC]$. Thus, the variation of the absorbance A with [DMPC] is given by:

$$A=\frac{A_W+A_L K_L[DMPC]}{1+K_L[DMPC]}. \quad (1)$$

As the total absorbance of the partitioning molecule as well as its absorbance in aqueous solution, A_W are known, the limit absorption in the lipid environment, A_L, and the binding constant can be estimated from an *A vs.* [DMPC] plot by a nonlinear least-square analysis of the data. An analogous equation can be drawn [39] to calculate the binding constant from the plot of fluorescence intensity, I_F, data *vs.* [DMPC].

The values obtained at the two pHs are not significantly different: $K_L=(3.2\pm0.5)\times10^4$ M^{-1} at pH=3 and $K_L=(2.0\pm0.5)\times10^4$ M^{-1} at pH=7.

Data from literature show that a neutral chlorin with ring substitutions in *meso*-positions has a quite higher binding constant ($K_L\approx114$ mM^{-1}), [40] which must be not only due to differences in the buffer and lipid nature but also due to the fact that this porphyrin does not aggregate in aqueous solutions in contrast with PPhe. The same authors reported that the cationic meso-tetra(*N*-methyl-4-pyridyl) porphyrin (TMpyP) incorporates into lipid vesicles ($K_L\approx6$ mM^{-1}) whereas the anionic meso-tetra(4-carboxyphenyl) porphyrin (at pH=7.3) does not. Comparatively, protoporphyrin IX with a quite different structure with two propionic acids attached on the same side of the ring deprotonated at pH=7.3 presents a much higher binding constant ($K_L\approx110$ mM^{-1}).

These results suggest that several factors contribute to porphyrin incorporation in membranes. The amphiphilic character of the dye (as in protoporphyrin) takes advantage of the nature of the lipid membrane allowing for the hydrophobic core of the porphyrins to be buried in contact with the lipid alkyl chain while the charged substituent groups interact with the charged polar head of the lipid. Previous studies using TCPP with four negatively charged phenylcarboxylic groups symmetrically placed showed no binding to lipid vesicles [40]. In the case of PPhe incorporation can be facilitated by the presence of the aminosulfonyl groups and the hydrophobic nature of the phenylalanine groups, in an environment which leads to no charge separation *i.e.* increases pK_a of carboxylic groups and therefore these remain uncharged.

3.3. TSPP interaction with DMPC vesicles

pH=7: At physiological conditions TSPP is a tetra-anion and from what was just discussed in the previous section, it is not expected to incorporate in the DMPC bilayer. In fact, apart from an increase in the solution turbidity due to the increase in vesicle concentration, absorption spectra remain identical in the range of [DMPC] used (up to 0.5 mM). In the same way, fluorescence spectra obtained upon excitation at 425 nm show some quenching only at high [DMPC] (above 0.25 mM). The fluorescence excitation spectra are similar to absorption at all studied concentrations confirming the absence of incorporation of TSPP in DMPC vesicles. TCPP and TSPP have the four negatively charged groups in a symmetrical placing around the π-system, thus preventing their incorporation.

pH=2.5: At pH=2.5, besides the four negative peripheral sulfonate groups also the two nitrogens in the inner tetrapyrrole are charged. Data from Brault et al. [41] showed that protonation of one inner nitrogen was sufficient to prevent incorporation of HP into lipid vesicles. From this, we could anticipate that TSPP with symmetrical negative groups and protonated inner nitrogens would not incorporate into DMPC bilayers. Although incorporation does not seem to occur, data obtained in this system show markedly differences in TSPP spectra upon addition of DMPC.

3.3.1. Absorption spectra

The absorbance in the Soret band region, which has a maximum at 435 nm characteristic of protonated inner nitrogens, decreases together with the appearance of a new band at around 489 nm which increases following the concomitant increase in [DMPC] until up to 0.25 mM, Fig. 4A. Similarly, in the Q-band region the absorbance at 643 nm decreases and a new band appears around 705 nm that increases at the expenses of the other until [DMPC]=0.25 mM. These two new bands were already assigned to J-aggregates of TSPP. Two isosbestic points relatively well defined are found at 448 and 662 nm which indicates the interconversion of two species. Similar values were obtained when varying the ionic strength with KCl [10,11] or varying protein concentration [18].

Noteworthy is the fact that at higher [DMPC] the absorbance of these two new bands decreases and there is a blue shift in the monomer Soret band from 435 to around 422 nm, similar to that already reported for TSPP in AOT RM at high water contents (e.g.:[water]/[AOT]=ω_0=50 [22]). The origin of the absorption band at 422 nm has been the subject of some controversy in literature. The band has been assigned to an H-aggregate of TSPP based on Raman data. However, the calculated value for the face-to-face packing in this type of aggregate is much larger than this experimental one at 422 nm. Moreover, Castriciano et

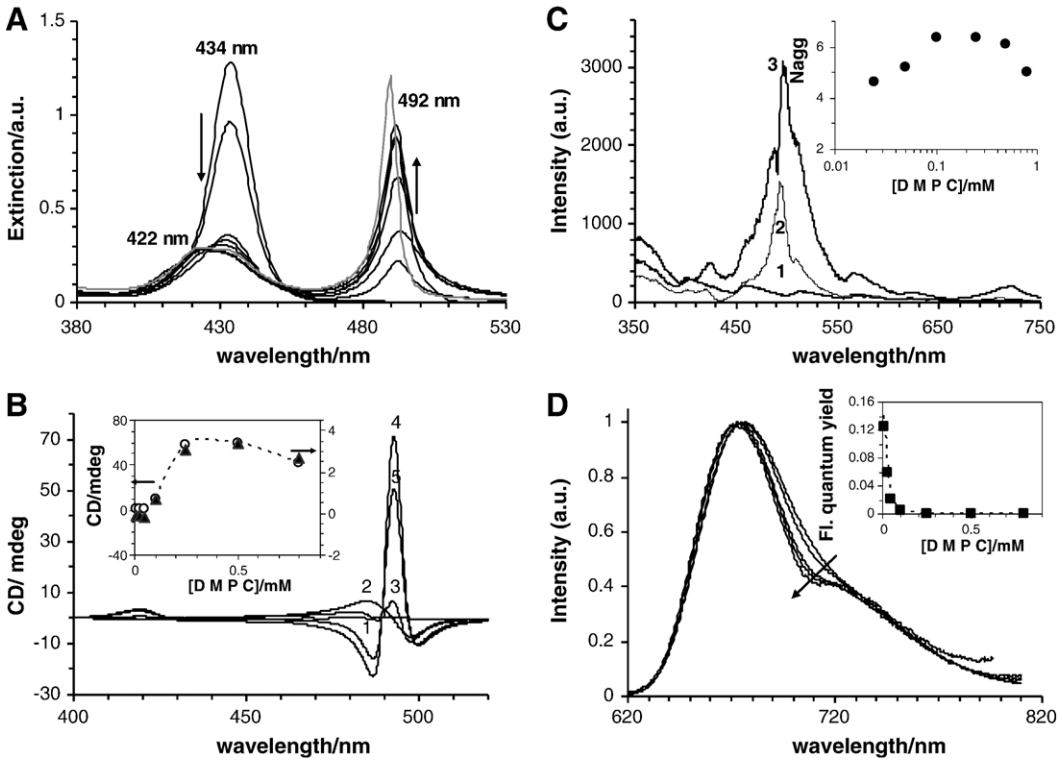

Fig. 4. Spectroscopic data of TSPP in aqueous solution at pH=2.5 in the presence of increasing [DMPC]=0–0.8 mM, indicated by the arrows: A) absorption (grey line: TSPP in AOT/*Iso*-octane/water ω_0=50); B) induced circular dichroism, *inset*: CD signal at 420 nm (●) and 492 nm (○); C) RLS signal of the (1) vesicle solution, (2) TSPP with [DMPC]=0.01 mM and (3) with [DMPC]=0.25 mM; *inset*: spectroscopic number of monomers in TSPP J-aggregate; D) normalized fluorescence emission, λ_{exc}=410 nm, *inset*: fluorescence quantum yield. [TSPP]=2 μM; *T*=32 °C.

al. [21] obtained essentially the same predominant lifetime upon TSPP excitation at 424 nm or 490 nm. Thus, it seems more plausible to attribute both bands to the splitting of TSPP B-band as a consequence of symmetry lowering of the porphyrin macrocycle in the aggregates [22]. Additional evidence may be obtained from CD measurements.

3.3.2. Induced circular dichroism

Circular dichroism, CD, the difference in the absorption of right and left circularly polarized light, arises from the chirality of a molecular architecture. This chirality can arise from either the structure of individual molecules or from the chiral packing of molecules into larger aggregates.

TSPP is a symmetrical molecule and does not yield CD signal in the visible range at the conditions above studied of pH and concentration, as shown in Fig. 4B. However, an intense signal in the absorption region of the J-aggregate (492 nm) and a rather weak one in the blue region (around 422 nm) of the monomer Soret band are detected which increase upon DMPC addition. This is indicative of an asymmetrical perturbation of the molecule. Bisignate CD signals obtained, Fig. 4B, are indicative that both transitions are degenerate. In spite of a much more intense CD signal in the 492 nm region, inset Fig. 4B, a similar pattern is observed in 422 nm upon increase of DMPC concentration which is in favor of a common origin for the two bands as proposed before. The order of the bands are indicative of the orientation of the adjacent units, hence, the negative band at longer wavelength and the positive at shorter wavelength are indicative of a left-handed orientation. This is different from that presented by TSPP J-aggregates induced in aqueous pools of AOT reverse micelles or in HSA, thus indicating that these systems induce a geometrically arrangement distinct from that induced by DMPC vesicles. In fact, Maiti et al. [42] showed that the macroscopic appearance of a linear arrangement of J-aggregates induced by K^+ was a fiber-like structure whereas a helical arrangement was proposed for J-aggregates induced by CTAB molecules.

3.3.3. Spectroscopic aggregate size

Although the physical size and the number of porphyrin units involved in the aggregate may be large, exciton theory allows for the calculation of the spectroscopic aggregation number, *N*, from the spectral width of the absorption band of the J-aggregate, this being proportional to $N^{-1/2}$. By using a previously described procedure [22,43] RLS data were used to withdraw the scattering contribution from the absorption spectra, which in the red portion of the aggregate absorption is rather significant and hence, calculate the *N* values from the corrected bandwidth of the aggregate. This number represents the number of adjacent molecules that are collectively excited. The values obtained are shown in the inset of Fig. 4C and give lower values as compared to those obtained in AOT RM but similar to those reported in CTAB micelles. The possibility of defect states in the molecular arrangement was raised to justify

these lower values of N [20]. Perhaps the inner aqueous pool of AOT RM is a more controlled environment less prone to dynamical changes in the template as it is the case of the surfaces of micelles or vesicles.

3.3.4. Steady-state and time-resolved fluorescence

The fluorescence obtained upon excitation at 425 nm shows a single band centered around 675 nm, which is quenched upon increase of [DMPC] until it reaches a plateau at [DMPC] ≥ 0.25 mM, Fig. 4D. From previous data we determined a fluorescence quantum yield of 0.14 for TSPP protonated monomer in aqueous solution [18] whereas the same value for J-aggregates is significantly lower, 10^{-3} [44]. In the presence of DMPC, global fluorescence quantum yield of TSPP obtained upon excitation at 425 nm decreases drastically, inset Fig. 4D, as expected, reflecting the formation of J-aggregates at the expenses of the monomer.

When the 490 nm absorption band exists, fluorescence spectra depend on excitation wavelength. Upon excitation at such wavelength the band peak at 675 nm is replaced by a new maximum around 720 nm which corresponds to the fluorescence of J-aggregates and therefore has low intensity but increases concomitantly with addition of more DMPC since more aggregates are formed.

Time resolved measurements were performed upon excitation at 638 nm and collected in the emission range of 667–722 nm. In the absence of lipid vesicles, the fluorescence decay is monoexponential with a fluorescence lifetime $\tau_F = 3.83 \pm 0.02$ ns, which agrees well with data published in literature [18,21,44]. In the presence of DMPC, the decays become bi-exponential and, on average, τ_F decreases until reaching a plateau at [DMPC] > 0.25 mM. A global analysis fitting of the data shows that the contribution of the longer component, assigned to TSPP protonated monomer, decreases as [DMPC] increases, by opposition to the shorter one which can be associated to the aggregated species of TSPP. In fact, upon excitation at 490 nm (J-aggregate absorption) and collecting emission in the whole spectrum, we obtained a maximal contribution of 90% (with [DMPC] = 0.5 mM) from a sub-picosecond component $\tau_1 = 0.07 \pm 0.04$ ns and 10% of a longer one ($\tau_2 = 3.1 \pm 0.2$ ns) due to some overlap from the monomer emission. This seems in agreement with literature data, where a value of 0.1 ± 0.03 ns was obtained for TSPP J-aggregate in CTAB micelles [20]. In water at pH = 1, a tri-exponential decay with $\tau_1 = 0.055$ ns (75%), $\tau_2 = 0.36$ ns (15%) and $\tau_3 = 3.4$ ns (10%), was reported.

3.3.5. FLIM

Fluorescence lifetime imaging spectroscopy (FLIM) allows the lifetimes of one or more fluorophores to be spatially resolved and can be used to provide information about the state of the fluorescent species and their microenvironment, since the fluorescence lifetime is sensitive to environmental conditions such as pH, viscosity, polarity and interactions with other molecules as well as aggregation state.

A spin-coated sample of aqueous TSPP shows a rather uniform picture with a single exponential decay with $\tau_F = 4.95$ ns, Fig. 5A due to TSPP monomers adsorbed to the glass coverslip.

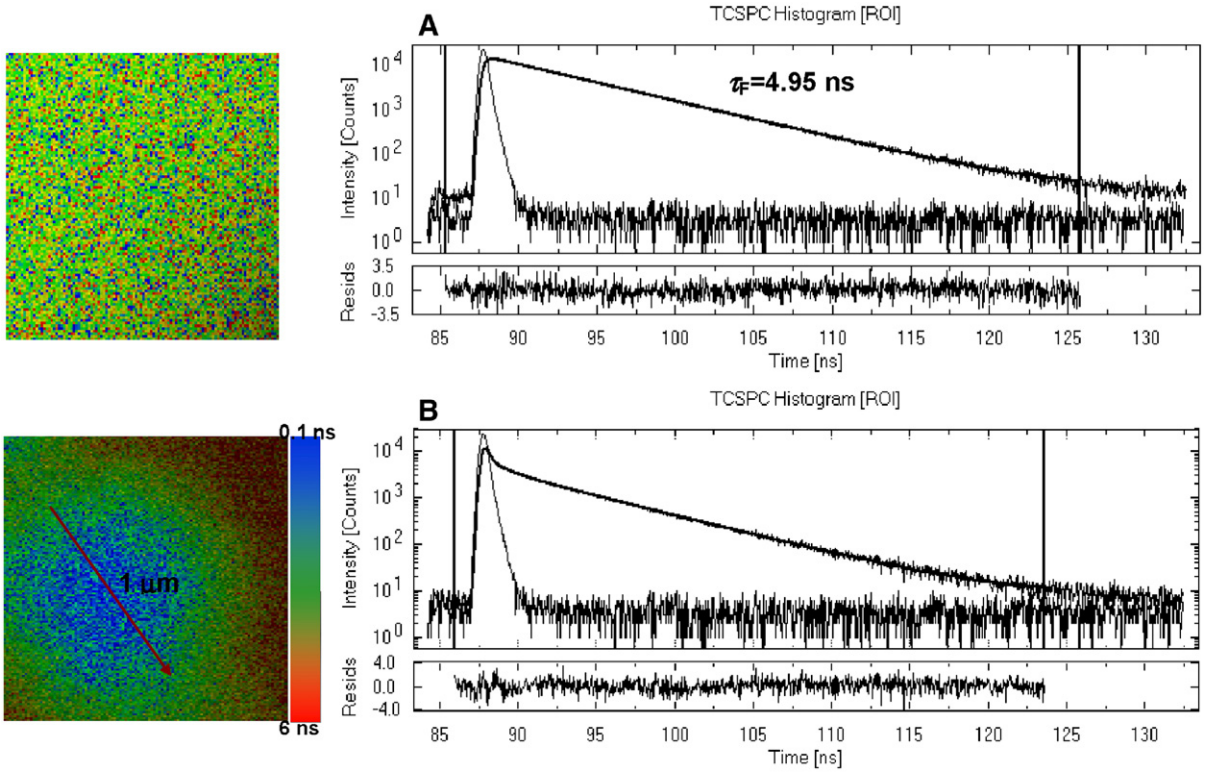

Fig. 5. Fluorescence lifetime image and fluorescence decays for (A) TSPP monomers and (B) TSPP J-aggregates in DMPC films spread on a glass cover slip.

A heterogeneous image 3×3 μm in XY direction (0.02 μm/pixel), is obtained from a spin-coated sample of TSPP in the presence of [DMPC]=0.25 mM, Fig. 5B. In the latter we may see approximately round spots with average sizes in the range of 800–1000 nm (optical resolution ~320 nm), which are much larger than those obtained in solution by DLS (without TSPP). PC vesicles were reported to flatten considerably upon adsorption to the glass (width-to-height-ratio ≈ 5) [45]. Besides, PC vesicles were also shown to fuse in glass substrate governed by pH and ionic strength [46], thus contributing to larger adsorbed round structures. Fluorescence decays obtained within such spots show that the main contribution (A=85%) is associated to a short fluorescence lifetime, τ_F=0.112 ns, which may safely be attributed to the J-aggregates fluorescence resulting from interaction of TSPP with the DMPC vesicles. Under analogous excitation and emission conditions, we were not able to detect the short lifetime for TSPP in DMPC solution due to the fact that fluorescence quantum yield from the prevailing monomers in solution (ϕ_F ~ 0.14 [18]) is much more efficient than that of the J-aggregate (ϕ_F ~ 0.001 [44]).

The longer lifetime is similar to that obtained in the absence of DMPC and assigned to the monomer adsorbed. An intermediate lifetime is probably associated to some less ordered aggregates induced upon film formation on the glass.

4. Conclusions

We have presented spectroscopic as well as photophysical data for two water-soluble porphyrins regarding their possible association with DMPC vesicles.

PPhe, a free base porphyrin with aminosulfonyl groups linked to an aromatic amino acid, phenylalanine, presented a complex aggregation pattern in aqueous solution strongly dependent on the pH. Under very acidic media, the predominant diprotonated PPhe coexists with some nonspecific nonfluorescent aggregates. However, upon pH increase and taking into account the spectroscopic data, a small dimension aggregate, a dimer in a co-facial arrangement predominates due to π–π interactions between porphyrin macrocycles and possible intramolecular H-bonds which involve the sulfonamide groups. Nevertheless, this porphyrin associates to the DMPC bilayer as a noncharged monomer regardless the pH of the aqueous solution. The combination of these studies with those in cells is important to envisage the potential application of PPhe as photosensitizer.

On the other hand, TSPP a monomer in solution does not incorporate within DMPC vesicles at any of the two prototropic forms studied. However, TSPP J-aggregates are induced at the vesicle surface under acidic conditions. In the case of the latter, protonation of the macrocycle together with peripheral anionic substituents are unfavorable conditions for binding to DMPC but adequate for forming highly ordered aggregates. The ability of these vesicles to induce such aggregates opens up the possibility for their application in nonlinear optics. Besides, further exciton characterization of porphyrin self-assembly may serve for a better understanding of aggregates in photosynthetic organisms.

Acknowledgments

This work was supported by Project POCI/QUI/57387/2004 and 3° Quadro Comunitário de Apoio (FEDER). The authors thank Professor J.M.G. Martinho for the use of DLS equipment and Prof. João Costa Pessoa for the use of the spectropolarimeter. S.M. Andrade thanks FCT for SFRH/BPD/24367/2005 grant and R. Teixeira thanks a grant from Pluriannual Project/CQE.

References

[1] D. Gust, T.A. Moore, A.L. Moore, Mimicking photosynthetic solar energy transduction, Acc. Chem. Res. 34 (2001) 40–48.
[2] H. van Amerongen, L. Valkunas, R. van Grondelle, Photosynthetic Excitons, World Scientific Publishing Co Pte. Ltd, Singapore, 2000.
[3] T. Yamaguchi, T. Kimura, H. Matsuda, T. Aida, Macroscopic spinning chirality memorized in spin-coated films of spatially designed dendritic zinc porphyrin J-aggregates, Angew, Chem. Int. Ed. 43 (2004) 6350–6355.
[4] K. Misawa, T. Kobayashi, Ultrafast exciton and excited-exciton dynamics in J-aggregates of three-level porphyrin molecules, J. Chem. Phys. 110 (1999) 5844–5850.
[5] E.G. McRae, M. Kasha, Enhancement of phosphorescence ability upon aggregation of dye molecules, J. Chem. Phys. 28 (1958) 721–722.
[6] D.A. Higgins, P.F. Barbara, Excitonic transitions in J-aggregates probed by near-field scanning optical microscopy, J. Phys. Chem. 99 (1995) 3–7.
[7] A.S. Tatikolov, S.M.B. Costa, Effects of normal and reverse micellar environment on the spectral properties, isomerization and aggregation of a hydrophilic cyanine dye, Chem. Phys. Lett. 346 (2001) 233–240.
[8] C. Spitz, C. Knoester, A. Ouart, S. Daehne, Polarized absorption and anomalous temperature dependence of fluorescence depolarization in cylindrical J-aggregates, Chem. Phys. 275 (2002) 271–284.
[9] O. Ohno, Y. Kaizu, H. Kobayashi, J-aggregate formation of a water-soluble porphyrin in acidic aqueous-media, J. Chem. Phys. 99 (1993) 4128–4139.
[10] N.C. Maiti, M. Ravikanth, S. Mazumdar, N. Periasamy, Fluorescence dynamics of noncovalently linked porphyrin dimers and aggregates, J. Phys. Chem. 99 (1995) 17192–17197.
[11] D.L. Akins, H.-R. Zhu, C. Guo, Absorption and Raman-scattering by aggregated meso-tetrakis(*p*-sulfonatophenyl)porphine, J. Phys. Chem. 98 (1994) 3612–3618.
[12] J.M. Ribó, J. Crusats, J.-A. Farrera, M.L. Valero, Aggregation in water solutions of tetrasodium diprotonated meso-tetrakis(4-sulfonatophenyl) porphyrin, J. Chem. Soc., Chem. Commun. 6 (1994) 681–682.
[13] R. Rubires, J. Crusats, Z. El-Hachemi, T. Jaramillo, M. López, E. Valls, J.-A. Farrera, J.M. Ribó, Self-assembly in water of the sodium salts of meso-sulfonatophenyl substituted porphyrins, New J. Chem. 23 (1999) 189–198.
[14] F. Mallamace, N. Micali, S. Trusso, L.M. Scolaro, A. Romeo, A. Terracina, R.F. Pasternack, Experimental evidence for self-similar structures in the aggregation of porphyrins in aqueous solutions, Phys. Rev. Lett. 76 (1996) 4741–4744.
[15] P.J. Collings, E.J. Gibbs, T.E. Starr, O. Vafek, C. Yee, L.A. Pomerance, R.F. Pasternack, Resonance light scattering and its application in determining the size, shape, and aggregation number for supramolecular assemblies of chromophores, J. Phys. Chem., B 103 (1999) 8474–8481.
[16] S.C.M. Gandini, E.L. Gelamo, R. Itri, M. Tabak, Small angle X-ray scattering study of meso-tetrakis (4-sulfonatophenyl) porphyrin in aqueous solution: a self-aggregation model, Biophys. J. 85 (2003) 1259–1268.
[17] I.E. Borissevitch, T.T. Tominaga, H. Imasato, M. Tabak, Fluorescence and optical absorption study of interaction of two water soluble porphyrins with bovine serum albumin. The role of albumin and porphyrin aggregation, J. Lumin. 69 (1996) 65–76.
[18] S.M. Andrade, S.M.B. Costa, Spectroscopic studies on thr interaction of a water soluble porphyrin with two drug carrier proteins, Biophys. J. 82 (2002) 1607–1619.

[19] S.M. Andrade, S.M.B. Costa, Aggregation kinetics of meso-tetrakis(4-sulfonatophenyl) porphine in the presence of proteins: temperature and ionic strength effects, J. Fluoresc. 12 (2002) 77–82.
[20] N.C. Maiti, S. Mazumdar, N. Periasamy, J- and H-aggregates of porphyrin-surfactant complexes: time-resolved fluorescence and other spectroscopic studies, J. Phys. Chem., B 102 (1998) 1528–1538.
[21] M.A. Castriciano, A. Romeo, V. Villari, N. Angelini, N. Micali, L.M. Scolaro, Aggregation behavior of tetrakis (4-sulfonatophenyl) porphyrin in AOT/water/decane microemulsions, J. Phys. Chem., B 109 (2005) 12086–12092.
[22] S.M. Andrade, S.M.B. Costa, Spectroscopic studies of water-soluble porphyrins with protein encapsulated in bis(2-ethylhexyl)sulfosuccinate (AOT) reverse micelles: aggregation versus complexation, Chem. Eur. J. 12 (2006) 1046–1057.
[23] P.M.R. Paulo, S.M.B. Costa, Non-covalent dendrimer–porphyrin interactions: the intermediacy of H-aggregates? Photochem. Photobiol. Sci. 2 (2003) 597–604.
[24] M.Y. Choi, J.A. Pollard, M.A. Webb, J.L. McHale, Counterion-dependent excitonic spectra of tetra(*p*-carboxyphenyl)porphyrin aggregates in acidic aqueous solution, J. Am. Chem. Soc. 125 (2003) 810–820.
[25] J.Y. Winum, J.M. Dogne, A. Casini, X. de Leval, J.L. Montero, A. Scozzafava, D. Vullo, A. Innocenti, C.T. Supuran, Carbonic anhydrase inhibitors: synthesis and inhibition of cytosolic membrane-associated carbonic anhydrase isozymes I, II, and IX with sulfonamides incorporating hydrazino moieties, J. Med. Chem. 48 (2005) 2121–2125.
[26] S.M. Andrade, C. Teixeira, D.M. Togashi, S.M.B. Costa, A.J.F.N. Sobral, Self-association of free base porphyrins with aminoacid substituents in AOT reverse micelles, J. Photochem. Photobiol. A Chem. 178 (2006) 225–235.
[27] A.J.F.N. Sobral, S. Eleouet, N. Rousset, A.M.d'A.R. Gonsalves, O. Le Meur, L. Bourré, T. Patrice, New sulfonamide and sulfonic ester porphyrins as sensitizers for photodynamic therapy, J. Porphy. Phthalocyanines 6 (2002) 456–462.
[28] H.S. Han, H. Kim, Spontaneous fragmentation of dimyristoylphosphatidylcholine vesicles into a discoidal form at low pH, J. Biochem. 115 (1994) 26–31.
[29] M.A.R.B. Castanho, N.C. Santos, L.M.S. Loura, Separating the turbidity spectra of vesicles from the absorption spectra of membrane probes and other chromophores, Eur. Biophys. J. 26 (1997) 253–259.
[30] P.M.R. Paulo, R. Gronheid, F.C. De Schryver, S.M.B. Costa, Porphyrin–dendrimer assemblies studied by electronic absorption spectra and time-resolved fluorescence, Macromolecules 36 (2003) 9135–9144.
[31] D.M. Togashi, S.M.B. Costa, A.J.F.N. Sobral, Lipophilic porphyrin microparticles induced by AOT reverse micelles — a fluorescence lifetime imaging study, Biophys. Chem. 119 (2006) 121–126.
[32] S.E. Clarke, C.C. Wamser, H.E. Bell, Aqueous complexation equilibria of meso-tetrakis(4-carboxyphenyl)porphyrin with viologens: evidence for 1:1 and 1:2 complexes and induced porphyrin dimerization, J. Phys. Chem., A 106 (2002) 3235–3242.
[33] H. Schneckenburger, K. Koenig, K. Kunzi-Rapp, C. Westphal-Froesch, A. Rueck, Time-resolved in vivo fluorescence of photosensitizing porphyrins, J. Photochem. Photobiol., B Biol. 21 (1993) 143–147.
[34] M. Yamashita, M. Nomura, S. Kobayashi, T. Sato, K. Haizawa, Picosecond time-resolved fluorescence spectroscopy of hematoporphyrin derivatives, IEEE J. Quantum Electron. 20 (1984) 1363–1369.
[35] J.H. Fuhrhop, C. Demoulin, C. Boettcher, J. Koning, U. Siggel, Chiral micellar porphyrin fibers with 2-aminoglycosamide head groups, J. Am. Chem. Soc. 114 (1992) 4159–4165.
[36] L.M. Scolaro, M. Castriciano, A. Romeo, S. Patane, E. Cefali, M. Allegrini, Aggregation behavior of protoporphyrin IX in aqueous solutions: clear evidence of vesicle formation, J. Phys. Chem., B 106 (2002) 2453–2459.
[37] R.F. Pasternack, P.J. Collings, Resonance light-scattering — a new technique for studying chromophore aggregation, Science 269 (1995) 935–939.
[38] J. Milhaud, New insights into water-phospholipid model membrane interactions, Biochim. Biophys. Acta, Biomembr. 1663 (2004) 19–51.
[39] Z. Huang, R.P. Haugland, Partition coefficients of fluorescent probes with phospholipids membranes, Biochem. Biophys. Res. Commun. 181 (1991) 166–171.
[40] M. Kepczynski, R.P. Pandian, K.M. Smith, B. Ehrenberg, Do liposome-binding constants of porphyrins correlate with their measured and predicted partitioning between octanol and water? Photochem. Photobiol. 76 (2002) 127–134.
[41] D. Brault, C. Veverbizet, T. Ledoan, Spectrofluorimetric study of porphyrin incorporation into membrane models — evidence for pH effects, Biochim. Biophys. Acta 857 (1986) 238–250.
[42] N.C. Maiti, S. Mazumdar, N. Periasamy, J- and H-aggregates of porphyrins with surfactants: fluorescence, stopped flow and electron microscopy studies, J. Porphy. Phthalocyanines 2 (1998) 369–376.
[43] M.A. Castriciano, A. Romeo, V. Villari, N. Micali, L.M. Scolaro, Nanosized porphyrin J-aggregates in water/AOT/decane microemulsions, J. Phys. Chem., B 108 (2004) 9054–9059.
[44] A. Miura, Y. Shibata, H. Chosrowjan, N. Mataga, N. Tamai, Femtosecond fluorescence spectroscopy and near-field spectroscopy of water-soluble tetra(4-sulfonatophenyl)porphyrin and its J-aggregate, J. Photochem. Photobiol., A Chem. 178 (2006) 192–200.
[45] H. Schonherr, J.M. Johnson, P. Lenz, C.W. Frank, S.G. Boxer, Vesicle adsorption and lipid bilayer formation on glass studied by atomic force microscopy, Langmuir 20 (2004) 11600–11606.
[46] P.S. Cremer, S.G. Boxer, Formation and spreading of lipid bilayers on planar glass supports, J. Phys. Chem., B 103 (1999) 2554–2559.